Counting loop diagrams: computational complexity of higher-order amplitude evaluation[*]

E. van Eijk[a], R. Kleiss[b], A. Lazopoulos[c]

HEFIN, University of Nijmegen, Nijmegen, the Netherlands

Abstract. We discuss the computational complexity of the perturbative evaluation of scattering amplitudes, both by the Caravaglios–Moretti algorithm and by direct evaluation of the individual diagrams. For a self-interacting scalar theory, we determine the complexity as a function of the number of external legs. We describe a method for obtaining the number of topologically inequivalent Feynman graphs containing closed loops, and apply this to 1- and 2-loop amplitudes. We also compute the number of graphs weighted by their symmetry factors, thus arriving at exact and asymptotic estimates for the average symmetry factor of diagrams. We present results for the asymptotic number of diagrams up to 10 loops, and prove that the average symmetry factor approaches unity as the number of external legs becomes large.

1 Introduction

With the advent of high-energy colliders such as LHC and TESLA, high-multiplicity final states will become ever more relevant, increasing the need for efficient evaluation of complicated multi-leg amplitudes. Performing such calculations by a direct evaluation of all relevant Feynman graphs is computationally hard in the sense that the number of graphs increases with N roughly as $N!$, the total number of external legs. For example, the $2 \to 8$ purely gluonic amplitude in QCD contains 10.5 million Feynman graphs at the tree level; and one may expect that loop corrections (described by many more diagrams) will also be important. A computational breakthrough has been achieved by the introduction of the Caravaglios–Moretti (CM) algorithm [1], in which the Schwinger–Dyson (SD) equations of the theory, rather than their decomposition in individual Feynman diagrams, are employed, thus leading to a complexity of order c^N (where c is a constant). Such methods, however, have to date only be formulated for the Born approximation. Barring a revolutionary new method for solving the SD equations including loop effects[1], the most straightforward approach would seem to use the vertices of the effective, rather than those of the bare, action. In such an approach the effective vertices with up to N legs have to be employed, which increases the complexity of the

CM algorithm. In order to assess the relative merit of the CM algorithm, it is therefore relevant to compare the computational complexity of the CM approach to the number of higher-order Feynman graphs. In Sect. 2, we calculate the number of individual diagrams, not weighted by their symmetry factors, in 0-, 1- and 2-loop level for four models of a self-interacting scalar theory. We also give the number of 1-particle irreducible graphs needed in the sequence. In Sect. 3 we give the number of diagrams, now weighted by their symmetry factors, for the four models, as they occur directly from the path integral. Section 4 contains asymptotic estimates, in the number of external legs, for weighted and unweighted graphs. In Sect. 5 we proceed in calculating the computational complexity of the CM algorithm in one and two loops. In Sect. 6 we compare the efficiency of the CM algorithm to that of the individual-diagram approach.

2 Counting diagrams

We consider a self-interacting scalar theory with arbitrary vertices of the type φ^k, $k = 3, 4, \dots$ We define the "potential"

$$V(\varphi) = \sum_{k \geq 3} \epsilon_k \, \frac{\varphi^k}{k!} \,, \tag{1}$$

where ϵ_k is 1 if the φ^k interaction is present; otherwise it is zero. We shall specialize to a number of cases:

$$\varphi^3 \text{ theory} : V(\varphi) = \varphi^3/6 \,,$$
$$\varphi^4 \text{ theory} : V(\varphi) = \varphi^4/24 \,,$$
$$\text{gluonic QCD} : V(\varphi) = \varphi^3/6 + \varphi^4/24 \,,$$
$$\text{effective theory} : V(\varphi) = e^\varphi - 1 - \varphi - \varphi^2/2 \,; \tag{2}$$

[a] e-mail: ernsteij@sci.kun.nl
[b] e-mail: kleiss@sci.kun.nl
[c] e-mail: lazopoul@sci.kun.nl

[1] In informal discussions, all the experts agree that this would be a tremendous advance – but no-one has a clue on how to approach it.
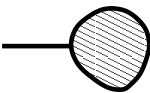
but alternative theories are easily implemented.

2.1 Counting tree diagrams

Tree diagrams can be conveniently counted by means of the SD equation. This hinges on the fact that, at the tree level, all diagrams have unit symmetry factor. The counting of tree diagrams has been described in detail in [2–4], and here we briefly recapitulate these results. Let us denote by $a(n)$ the *number of Feynman tree diagrams* contributing to the $1 \rightarrow n$ amplitude, and define the generating function
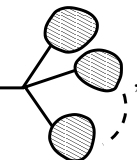
$$\phi_0(x) = \sum_{n \geq 1} \frac{x^n}{n!} \, a(n) \, . \tag{3}$$

Pictorially, we denote this as

$$\phi_0(x) = \text{---}\bigcirc \tag{4}$$

By considering the alternatives when entering the blob from the left, we easily see that

$$\phi_0(x) = \sum_{k \geq 2} \epsilon_{k+1} \quad , \tag{5}$$

where the right-hand side contains k blobs. This implies that $\phi_0(x)$ obeys the equation

$$\phi_0(x) = x + V'(\phi_0(x)) \, . \tag{6}$$

Since $V(\varphi)$ is of order $\mathcal{O}(\varphi^3)$, this SD equation can easily be iterated starting with $\phi_0(x) = 0$, and the desired $a(n)$ can be read off once the iteration has proceeded far enough. Notice that

$$V''(\phi_0(x)) = 1 - \frac{1}{\phi_0'(x)} \, ,$$

$$V^{(p)}(\phi_0(x)) = \frac{1}{\phi_0'(x)} \frac{\mathrm{d}}{\mathrm{d}x} V^{(p-1)}(\phi_0(x)) \quad (p \geq 3) \, , \tag{7}$$

so that the higher derivatives of $V(\phi_0(x))$ are completely expressed in terms of $\phi_0'(x)$ and *its* derivatives.

The asymptotic behavior of $a(n)$ for large n is determined by the singularity structure of $\phi_0(x)$. Since $\phi_0(x)$ cannot reach infinity for finite values of x, the singularities take the form of branch cuts, where $\phi_0(x)$ remains continuous but (as it turns out in all cases studied so far) $\phi_0'(x)$ diverges. We have

$$x = \phi_0 - V'(\phi_0) \quad \Rightarrow \quad \frac{\mathrm{d}x}{\mathrm{d}\phi_0} = 1 - V''(\phi_0) \, , \tag{8}$$

and the dominant singularity is reached for that value ϕ_c for which $V''(\phi_c) = 1$ and

$$x_c = \phi_c - V'(\phi_c) \tag{9}$$

theory	ϕ_c	x_c	C
φ^3	1	$1/2$	$\sqrt{2}$
φ^4	$\sqrt{2}$	$\sqrt{8/9}$	$2^{1/4}$
gQCD	$-1 + \sqrt{3}$	$\sqrt{3} - 4/3$	$(4/3)^{1/4}$
effective	$\log(2)$	$2\log(2) - 1$	1

is closest to the origin[2]. This value is always located on the positive real axis, where $\phi_0(x)$ is concave and monotically increasing for $x < x_c$. Taylor expansion then gives the structure of the branch cut:

$$\phi_0(x) \sim \phi_c - \sqrt{\frac{2x_c}{V^{(3)}(\phi_c)}} \left(1 - \frac{x}{x_c}\right)^{1/2} \, , \tag{10}$$
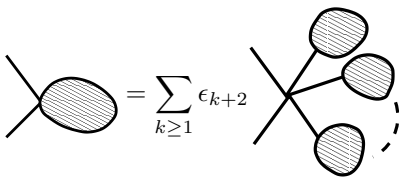
from which we conclude that, for large n,

$$a(n) \sim \sqrt{\frac{x_c}{2\pi V^{(3)}(\phi_c)}} \frac{n!}{n^{3/2} x_c^n} = \frac{C}{\sqrt{4\pi}} \frac{n!}{n^{3/2} x_c^{n-1/2}} \, . \tag{11}$$

with $C \equiv \sqrt{2/V^{(3)}(\phi_c)}$. In Table 1 we give the relevant numbers for the four case theories.

2.2 Counting 1-loop diagrams

When closed loops are introduced, an SD-type equation itself cannot be used to count the number of *topologically inequivalent* graphs. This stems from the fact that the SD-type equations are *local* in the sense that they only consider (in a recursive manner) what happens at a single vertex of a diagram, while the topology of a graph containing closed loops is a *global* property of the whole graph. Instead, one has to settle for an order-by-order and topology-by-topology treatment.

Every 1-loop diagram can be viewed as a single closed loop, to which tree-diagram pieces (which we call *leaves*) are attached. From

$$\bigotimes = \sum_{k \geq 1} \epsilon_{k+2} \tag{}$$

$$= \sum_{k \geq 1} \frac{\epsilon_{k+2}}{k!} \phi_0(x)^k = V''(\phi_0(x)) \equiv v \, , \tag{12}$$

where the sum has k blobs again, and we have introduced the shorthand notation v, we see immediately that the number of 1-loop graphs can be completely expressed in

---

[2] Here, we disregard the possibility that there are several such values, arising from a symmetry of the potential such as in the case of theories with only φ^m interactions ($m \geq 4$). These cases are treated in detail in [6] and references therein. The asymptotic results given here are "coarse-grained".

terms of v. The generating function of $L_1(n)$, the number of all 1-loop non-vacuum graphs with precisely n external legs, is given by attaching leaves to a closed loop in all possible ways:

$$\mathcal{L}_1(x) = \sum_{n \geq 1} \frac{x^n}{n!} L_1(n)$$

$$= \; \bigcirc\!\!\!\!\bigcirc \;+\; \bigcirc\!\!\!\!\bigcirc$$

$$+ \; \bigcirc\!\!\!\!\bigcirc \;+\; \bigcirc\!\!\!\!\bigcirc \;+\ldots \quad (13)$$

The standard combinatorics for collecting the various external legs into leaves and inspecting the symmetry properties of the resulting graphs show that a 1-loop graph with m leaves has precisely the "natural" symmetry factor $1/(2m)$, with two important exceptions: the graphs with one or two leaves have an additional symmetry since, for the 1-leave graph, the loop line may be flipped over, and for the 2-leave graph the two internal loop lines may be interchanged. This leads us to the strategy for computing the number of topologically inequivalent graphs.

(1) Write down the vacuum graphs, with their "natural" symmetry factor";
(2) attach leaves in all possible places;
(3) multiply by the order of the residual symmetry left over after the particular attachment.

Performing this program for the 1-loop case, we find

$$\mathcal{L}_1(x) = \frac{2}{2}v + \frac{2}{4}v^2 + \sum_{m \geq 3} \frac{1}{2m} v^m$$

$$= \frac{1}{2}v + \frac{1}{4}v^2 - \frac{1}{2}\log(1 - v)$$

$$= \frac{1}{2}v + \frac{1}{4}v^2 + \frac{1}{2}\log(\phi_0'(x)). \quad (14)$$

The number of 1-loop diagrams with n external legs is given in Table 2 for some theories.

2.3 Counting 2-loop diagrams

At the 2-loop level, there are three topologically different vacuum diagrams. These are

a: $\frac{1}{8}$, b: $\frac{1}{12}$, c: $\frac{1}{8}$, (15)

where we have indicated their "natural" symmetry factor. Since these graphs contain vertices, we must also accommodate leaves attaching themselves to vertices:

Table 2. The number of 1-loop diagrams with n external legs

N	φ^3	φ^4
1	1	0
2	2	1
3	7	0
4	39	7
5	297	0
6	2,865	145
7	33,435	0
8	457,695	6475
9	7,187,985	0
10	127,356,705	503,440
N	gQCD	effective
1	1	1
2	3	3
3	14	15
4	99	111
5	947	1,104
6	11,460	13,836
7	167,660	209,340
8	2,876,580	3,711,672
9	56,616,665	75,461,808
10	1,257,154,920	1,730,420,592

$= V^{(3)}(\phi(x)) - V^{(3)}(0),$

$= V^{(4)}(\phi(x)) - V^{(4)}(0). \quad (16)$

In case no leave happens to be attached, the expression for the vertices read, of course, $V^{(3)}(0)$ and $V^{(4)}(0)$, respectively. This prohibits, for instance, the occurrence of a 3-point vertex in a φ^4 theory. For each of the graphs we have to admit the possibility of zero, one, or more leaves on each line, and that of leaves on any vertex. For the determination of the residual symmetries it must be remembered that lines without leaves on them *may* be interchanged, and vertices without leaves *may* be interchanged, provided the "anchoring" of the graph to the external legs contained in every leaf present permits such an interchange. As a simple example, the vacuum graphs themselves, without any leaves on them, have a residual symmetry of precisely 8, 12, and 8, respectively, so that indeed they will be counted precisely one time. For graph (a) there are now $2 \times 3^2 = 18$ cases to be considered, and for (b) and (c) we have $2^2 \times 3^3 = 108$ cases. The results for their generating functions are

$$\mathcal{L}_2^{(a)}(x) = \frac{1}{8} V^{(4)}(\phi) \left[\left(1 + v + \frac{1}{1-v} \right)^2 + 4 \right],$$

$$\mathcal{L}_2^{(b)}(x) = \frac{1}{12} \left[\left(V^{(3)}(\phi) \right)^2 \left(2 + \frac{3}{1-v} + \frac{1}{(1-v)^3} \right) \right]$$

Table 3. Results for total number $L_2(n)$ of 2-loop graphs with precisely n external lines for our specific theories; see (18)

| N	φ^3	φ^4
0	2	1
1	3	0
2	10	3
3	58	0
4	465	42
5	4,725	0
6	57,900	1,485
7	829,080	0
8	13,570,515	97,335
9	249,789,015	0
10	5,105,239,650	10,210,200

N	gQCD	effective
0	3	3
1	6	7
2	29	35
3	217	273
4	2,214	2,876
5	28,365	38,034
6	436,780	604,320
7	7,847,420	11,202,156
8	161,048,720	237,187,552
9	3,715,400,500	5,645,523,408
10	95,156,789,700	149,180,360,320

$$+ \left(V^{(3)}(0)\right)^2 \left(2 + 3(1+v) + (1+v)^3\right)\Bigg],$$

$$\mathcal{L}_2^{(c)}(x) = \frac{1}{8}\left[\left(V^{(3)}(\phi)\right)^2 \frac{1}{1-v}\left(1 + v + \frac{1}{1-v}\right)^2 \right.$$

$$\left. + 4\left(V^{(3)}(0)\right)^2 (1+v)\right]. \tag{17}$$

The total number $L_2(n)$ of 2-loop graphs with precisely n external lines is therefore given via

$$\mathcal{L}_2(x) = \sum_{n \geq 0} \frac{x^n}{n!} L_2(n) = \mathcal{L}_2^{(a)}(x) + \mathcal{L}_2^{(b)}(x) + \mathcal{L}_2^{(c)}(x). \tag{18}$$

In Table 3 we give again the results for our specific theories.

The extension to three or more loops is a matter of establishing the vacuum diagrams. For the 3-loop case, however, there are 15 such graphs. Dressing them with leaves leads to a larger number of cases to be considered, ranging from 54 to 11,664 per graph.

2.4 Counting amputated diagrams

Loop diagrams containing tadpoles or seagulls are constant contributions to lower-order diagrams and are usually ignored. Moreover, diagrams containing self-energy loops on external legs are absorbed, during the renormalization procedure. Removing such diagrams from the above results is a simple task. One has to subtract all contributions from (a) diagrams with loops carrying zero or one vertex, and (b) diagrams carrying two vertices one of which is connected with an external leg while the other is a single propagator.

For the 1-loop case one has to subtract the first graph in (13), as a set of tadpole or seagul diagrams, as well as a contribution from graphs of the form
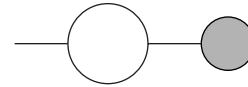
With these modifications the generating function reads

$$\mathcal{L}_1(x) = -\frac{1}{2}v + \frac{1}{4}v^2 - \frac{1}{2}\log(1-v) - x\phi_0(x)V^{(3)}(0). \tag{19}$$

The number of amputated 1-loop diagrams for our test theories is given in Table 4.

For 2-loop diagrams one has to consider separately each vacuum graph. All graphs containing loops with less than two vertices should be removed, as well as a variety of special cases which lead to non-amputated diagrams.

The generating functions for each of the three basic topologies becomes

$$\mathcal{L}_2^{(a)}(x) = \frac{1}{8}V^{(4)}(\phi)\left(\frac{v^2(2-v)^2}{(1-v)^2}\right)$$

$$- V^{(4)}(0)V^{(3)}(0)x\phi_0(x)$$

$$\mathcal{L}_2^{(b)}(x) = \frac{1}{12}\left[\left(V^{(3)}(\phi_0)\right)^2\left(\frac{6 - 12v + 9v^2 - 2v^3}{(1-v)^3}\right)\right]$$

$$- \frac{1}{12}\left(V^{(3)}(0)\right)^2\left[12x\phi_0 + \frac{6 - 3v^2 + 2v^3 + v^4}{1-v}\right]$$

$$- \left(V^{(4)}(0)\right)^2 x\phi_0(x) - V^{(3)}(0)V^{(3)}(\phi_0)$$

$$- V^{(3)}(0)V^{(4)}(0)2x\phi_0(x),$$

$$\mathcal{L}_2^{(c)}(x) = \frac{1}{8}\left[\left(V^{(3)}(\phi)\right)^2 \frac{v^2(2-v)^2}{(1-v)^3}\right] \tag{20}$$

$$- \frac{1}{8}V^{(3)}(\phi)V^{(3)}(0)x\frac{4v(2-v)}{(1-v)^2} + \left(V^{(3)}(0)\right)^2 \frac{4}{8}\frac{x^2}{1-v}.$$

Table 4. Number of amputated 1-loop diagrams for our test theories

N	φ^3	φ^4	gQCD	effective
3	1	0	4	4
4	12	3	39	43
5	117	0	437	502
6	1,290	75	5,800	6,916
7	16,425	0	90,450	111,660
8	239,400	3675	1,627,640	2,077,944
9	3,944,745	0	33,258,715	43,883,696
10	72,627,030	303240	761,405,820	1,037,955,824

Table 5. Exact number of 2-loop connected amputated diagrams for our test theories

N	φ^3	φ^4
3	4	0
4	63	9
5	870	0
6	12,945	460
7	212,940	0
8	3,874,815	35,315
9	77,605,290	0
10	1,700,078,625	4,090,800

N	gQCD	effective
3	28	37
4	457	600
5	7,285	9,760
6	128,675	177,160
7	2,552,165	3,617,824
8	56,538,055	82,588,784
9	1,387,411,690	2,089,438,256
10	37,407,699,175	58,096,995,744

Table 6. Numbers resulting from (21)

N	φ^3	φ^4	gQCD	effective
1	1	0	1	1
2	1	1	2	2
3	1	0	4	5
4	3	3	12	17
5	12	0	57	83
6	60	15	390	557
7	360	0	3,195	4,715
8	2,520	315	30,555	47,357
9	20,160	0	333,900	545,963
10	181,440	11,340	4,105,080	7,087,517

The exact number of 2-loop connected amputated diagrams for our test theories is given in Table 5.

2.5 Counting 1PI diagrams

The same methods as above can easily be employed in order to compute the number of 1-particle irreducible (1PI) diagrams. We simply restrict ourselves to the 1PI vacuum bubbles; and, since 1PI diagrams cannot have any vertex in their leaves, we simply replace $\phi_0(x)$ in the arguments of $V'', V^{(3)}, V^{(4)}, \dots$ by x. For the generating function of the 1PI 1-loop diagrams, we therefore have

$$\mathcal{L}_1^{1PI}(x) = \frac{1}{2}w + \frac{1}{4}w^2 - \frac{1}{2}\log(1-w), \quad w = V''(x). \quad (21)$$

The resulting numbers are given in Table 6.

Table 7. Same as Table 6; now see (22)

N	φ^3	φ^4	gQCD	effective
0	1	1	2	2
1	1	0	3	4
2	2	2	9	13
3	7	0	40	62
4	36	12	265	410
5	240	0	2,230	3,499
6	1,860	225	22,485	36,213
7	16,380	0	261,135	435,852
8	161,280	8,295	3,418,695	5,944,000
9	1,753,920	0	49,712,670	90,309,029
10	20,865,600	481,950	794,102,400	1,510,208,963

At the 2-loop level, we similarly find

$$\mathcal{L}_2^{1PI}(x) = \frac{1}{8}V^{(4)}(x)\left[\left(1 + w + \frac{1}{1-w}\right)^2 + 4\right]$$
$$+ \frac{1}{12}V^{(3)}(x)^2\left[2 + \frac{3}{1-w} + \frac{1}{(1-w)^3}\right] \quad (22)$$
$$+ \frac{1}{12}V^{(3)}(0)^2\left[2 + 3(1+w) + (1+w)^3\right].$$

Numbers are given in Table 7.

3 Counting with symmetry factors

The counting of diagrams including their symmetry factors is a somewhat simpler task, which can be performed on the basis of the path integral itself. In [5] this has been discussed in detail. However our approach here is somewhat different. One can expand the generating function of the number of connected diagrams perturbatively around $\varphi = 0$ and get a series in x (the source). Or, alternatively, one can expand perturbatively around the tree level 1-point function $\varphi = \phi_0$. This shift eliminates the source x in favour of the tree level 1-point function $\phi_0(x)$, and reveals the vacuum graph dressing procedure that we employed above.

3.1 Counting diagrams with symmetry factors

Consider the generating function for the number of disconnected diagrams of a scalar theory with arbitrary couplings and a source x:

$$Z(x) = N \int d\varphi \, \exp\left(-\frac{1}{\hbar}\left(\frac{1}{2}\varphi^2 - V(\varphi) + x\varphi\right)\right), \quad (23)$$

with $N = 1/\sqrt{2\pi\hbar}$. Expanding around the tree level approximation ϕ_0 of the 1-point function, i.e. setting $\varphi \to \phi_0 + \varphi$, and making use of the Schwinger–Dyson equation for $\phi_0(x)$ gives

$$Z(x) = N \, \exp\left(-\frac{1}{\hbar}S(\phi_0) + \frac{x\phi_0}{\hbar}\right)\int d\varphi \, e^{-\frac{1}{\hbar}\hat{S}(\varphi)}, \quad (24)$$

with

$$\hat{S}(\varphi) = \frac{1 - V''(\phi_0)}{2}\varphi^2 - \sum_{n=3}^{\infty} V^{(n)}(\phi_0)\frac{\varphi^n}{n!} \qquad (25)$$

The generating function of the number of connected diagrams is then

$$W(x) = \hbar \log(Z(x)) \qquad (26)$$

$$= -S(\phi_0) + x\phi_0 + \hbar \log\left(N\int \mathrm{d}\varphi e^{-\frac{1}{\hbar}\hat{S}(\varphi)}\right).$$

We see that it can be seen as a sum of the tree level part plus higher-order corrections. These corrections can be written as the generating function for the vacuum diagrams of a theory with action $\hat{S}(\varphi)$. The Feynman rules corresponding to this action can be read off directly:
(1) $\frac{1}{1 - V''(\phi_0)} = \phi_0'$ for every propagator.
(2) $V^{(n)}(\phi_0)$ for every n-point vertex.

Given the potential $V(\varphi)$ of the theory one can expand the vertex terms in the exponential of (26), calculate the Gaussian integrals and arrive at an expression for $W(x)$ that contains only $V''(\phi_0(x))$ and its derivatives. In this way, given the tree level 1-point function of the theory, one finds the number of graphs weighted by their symmetry factors to arbitrary order.

Writing $W(x)$ in an $\hbar$ expansion

$$W(x) = W_0(x) + \hbar W_1(x) + \hbar^2 W_2(x) + \dots \qquad (27)$$

and, performing the integral and collecting together the terms of the same order in $\hbar$, we see that the 1-loop diagrams are generated by

$$W_1(x) = \frac{1}{2}\log\left(\frac{1}{1 - V''(\phi_0)}\right) \qquad (28)$$

We can also find the generating function for the 2-loop diagrams

$$W_2(x) = \frac{1}{8}\frac{V^{(4)}(\phi_0)}{(1 - V''(\phi_0))^2} + \frac{5}{24}\frac{V^{(3)}(\phi_0)V^{(3)}(\phi_0)}{(1 - V''(\phi_0))^3}. \qquad (29)$$

The factor $\frac{1}{8}$ in front of the first term is the symmetry factor of the only 2-loop vacuum diagram with a 4-vertex (see (15a)). The factor $\frac{5}{24} = \frac{1}{8} + \frac{1}{12}$ is the sum of the symmetry factors of the two vacuum diagrams with two 3-vertices (see (15b,c))[3].

Writing the derivatives $V^{(m)}(\phi_0)$ in terms of derivatives of ϕ_0 (which can be done by differentiating the Schwinger–Dyson equation for ϕ_0) one arrives at

$$W_2(x) = \frac{1}{8}\frac{\phi_0'''}{(\phi_0')^2} - \frac{1}{6}\frac{(\phi_0'')^2}{(\phi_0')^3}. \qquad (30)$$

In Table 8 we give results for our four case theories in one loop.

---

[3] In fact one could even avoid performing the integral since the generating function for N loops is simply the sum of the vacuum graphs with N loops weighted by their symmetry factors using the Feynman rules for the $\hat{S}(\varphi)$ action given above. However, this presupposes that one knows what the symmetry factor of the specific vacuum diagram is.

Table 8. Results for our four case theories in one loop; see (30)

N	φ^3	φ^4	gQCD	effective
1	1/2	0	1/2	1/2
2	1	1/2	3/2	3/2
3	4	0	15/2	8
4	24	7/2	57	63
5	192	0	1,149/2	658
6	1,920	80	7,230	8,568
7	23,040	0	218,175/2	133,676
8	322,560	3,815	1,919,190	2,430,816
9	5,160,960	0	77,146,125/2	50,484,016
10	92,897,280	31,0940	871,927,770	1,178,963,856

Table 9. Same as Table 8: results for the four theories now in two loops

N	φ^3	φ^4
1	5/8	0
2	25/8	2/3
3	175/8	0
4	1,575/8	149/12
5	17,325/8	0
6	225,225/8	1,535/3
7	3,378,375/8	0
8	57,432,375/8	111,755/3
9	1,091,215,125/8	0
10	22,915,517,625/8	12,672,800/3
N	gQCD	effective
1	31/24	17/12
2	25/3	19/2
3	1,777/24	527/6
4	5,057/6	1,037
5	280,735/24	44,726/3
6	1,149,515/6	252,734
7	86,813,545/24	14,808,232/3
8	464,096,885/6	109,143,424
9	44,344,732,495/24	8,085,390,392/3
10	292,590,237,275/6	73,514,104,288

The results for the four theories in two loops are again collected in Table 9. Both in the 1- and 2-loop cases an intriguing pattern of denominators is apparent for large N values, which seems to persist (we have checked this for N up to 50).

The above procedure can easily be extended to higher-loop amplitudes as well, but since we have not computed the unweighted diagram sums we defer this discussion to the case of asymptotically large N.

3.2 Counting 1PI graphs

The generating function for the 1-particle irreducible diagrams of a theory weighted by their symmetry factors

Table 10. Number of irreducible diagrams weighted by their symmetry factors in the 1-loop case for the four test theories

	φ^3	φ^4	$\varphi^3 + \varphi^4$	effective
$N = 1$	1/2	0	1/2	1/2
$N = 2$	1/2	1/2	1	1
$N = 3$	1	0	5/2	3
$N = 4$	3	3/2	21/2	13
$N = 5$	12	0	57	75
$N = 6$	60	15	390	541
$N = 7$	360	0	3,195	4,683
$N = 8$	2,520	315	30,555	47,293
$N = 9$	20,160	0	333,900	545,853
$N = 10$	181,440	11,440	4,105,080	7,087,261

Table 11. Number of irreducible diagrams weighted by their symmetry factors in the 2-loop case for the four test theories

	φ^3	φ^4	$\varphi^3 + \varphi^4$	effective
$N = 1$	1/4	0	2/3	19/24
$N = 2$	1	5/12	41/12	101/24
$N = 3$	5	0	89/4	691/24
$N = 4$	30	21/4	709/4	5765/24
$N = 5$	210	0	1,660	56,659/24
$N = 6$	1,680	135	17,865	64,0421/24
$N = 7$	15,120	0	217,035	8,178,931/24
$N = 8$	151,200	5,775	2,936,745	116,422,085/24
$N = 9$	1,663,200	0	43,787,520	1,827,127,699/24
$N = 10$	19,958,400	368,550	713,163,150	31,336,832,741/24

can be obtained by the same prescription by substituting $\phi_0 = x$. Now, however, we have to take into account only the 1PI vacuum diagrams. In the 1-loop case the only vacuum graph is 1PI and the generating function is

$$W_1(x) = \frac{1}{2} \log \left(\frac{1}{1 - V''(x)} \right). \qquad (31)$$

In the 2-loop case we have to take into account the vacuum graph with one 4-vertex (see (15a)) and only one of the two vacuum graphs with three vertices (see (15b)) since the other one (see (15c)) is not 1PI. This alters the symmetry factor from $\frac{5}{24}$ to $\frac{1}{12}$. We get then

$$W_2(x) = \frac{1}{8} \frac{V^{(4)}(x)}{(1 - V''(x))^2} + \frac{1}{12} \frac{V^{(3)}(x)V^{(3)}(x)}{(1 - V''(x))^3}. \qquad (32)$$

We give in Table 10 the number of irreducible diagrams weighted by their symmetry factors in the 1-loop case for the four test theories.

We give in Table 11 the number of irreducible diagrams weighted by their symmetry factors in the 2-loop case for the four test theories.

4 Asymptotic estimates

It is fairly easy to estimate the number of diagrams, both with and without their symmetry factors, for asymptotically large N. As before, the asymptotic behavior of these numbers is governed by the analytic structure of their generating functions close to that singularity which is closest to the origin (that is, around $x \sim x_c$). There, we have

$$\phi_0'(x) \sim \frac{1}{2} C \left(x_c - x \right)^{-1/2}, \quad C = \left(2/V^{(3)}(\phi_c) \right)^{1/2}, \qquad (33)$$

where x_c, ϕ_c and C again depend on the theory. Let us first concentrate on the 1-loop diagrams. Since $v = 1 - 1/\phi_0'(x)$ has a square-root branch cut at the singular point, $\log(1-v)$ is more singular than v or v^2, and we have

$$\mathcal{L}_1(x) \sim \frac{1}{2} \log \left(\frac{C}{2\sqrt{x_c - x}} \right) = \mathcal{L}_1^{(s)}(x). \qquad (34)$$

We conclude that, for 1-loop diagrams, the *average symmetry factor* of a given diagram is asymptotically equal to 1. The number $K_1(N)$ of graphs contained in the 1-loop N-point amplitude is asymptotically given by

$$K_1(N) \sim \frac{1}{4} \frac{1}{(x_c)^N} \frac{N!}{N}. \qquad (35)$$

To illustrate the convergence of the weighted number of graphs to the unweighted number, we give the ratio of the coefficients of x^N in $\mathcal{L}_1^{(s)}(x)$ to those of $\mathcal{L}_1(x)$ as a function of N below, for the pure φ^3 theory. The other cases show a similar behavior[4], in which the asymptotic regime is approached as $1/\sqrt{N}$: this can also be easily checked from the exact form of $\mathcal{L}_1(x)$ close to the singularity; refer to Fig. 1.
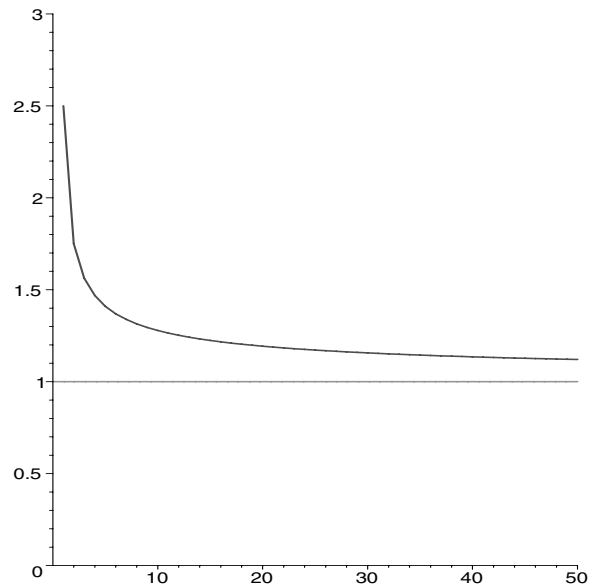

Fig. 1. Exact form of $\mathcal{L}_1(x)$ close to the singularity

---

[4] For the pure φ^4 theory, this holds in the "coarse-grained" approximation [6].

Table 12. First coefficients w_L

L	w_L	L	w_L
2	5 / 48	7	19675 / 6144
3	5 / 64	8	1282031525 / 88080384
4	1105 / 9216	9	80727925 / 1048576
5	565 / 2048	10	1683480621875 / 3623878656
6	82825 / 98304	11	13209845125 / 4194304

The asymptotic results for the higher-loop amplitudes can be established by the following reasoning. The leading contribution from each leave-dressed vacuum diagram is given by that part that has the highest degree of divergence as $x \to x_c$. From each line in the vacuum graph, this is a factor $1/(1 - v) = \phi_0'(x)$. Furthermore, from each k-point vertex in the vacuum graph the leading contribution comes from the limiting behavior of $V^{(k)}(\phi_0(x))$. Now, it is easily seen that, as $x \to x_c$,

$$V^{(3)}(\phi_0(x)) \sim \frac{2}{C^2} \quad \Rightarrow V^{(k)}(\phi_0(x)) \sim 0, \quad k \geq 4. \quad (36)$$

We conclude that the leading behavior of the number of unweighted graphs is given by those vacuum graphs that contain only 3-point vertices. To get the number of unweighted diagrams at the L-loop level, therefore, we first compute the normalized path integral for the pure φ^3 theory, using the usual perturbative interchange between expansion of the potential term and integration:

$$Z = N \int\limits_{-\infty}^{\infty} d\varphi \, \exp\left(-\frac{\mu}{2}\varphi^2 + \frac{\lambda}{6}\varphi^3\right)$$

$$= \sum_{n \geq 0} \frac{(6n)!}{(2n)!(3n)!(576)^n} \left(\frac{\lambda^2}{\mu^3}\right)^n. \quad (37)$$

The sum of all connected vacuum diagrams with interactions is then given by

$$W = \log(Z), \quad (38)$$

in the expansion of which the L-loop contribution ($L \geq 2$) is given by the term with λ^{2L-2}. In this expression, it suffices to replace λ by $2/C^2$ and μ by $1/\phi_0'(x)$. The result is

$$W = \sum_{L \geq 2} w_L \, C^{1-L} \, (x_c - x)^{3(1-L)/2}. \quad (39)$$

The first coefficients w_L are given in Table 12. The asymptotic result for $K_L(N)$, the number of unweighted diagrams contributing to the L-loop n-point amplitude is therefore given by

$$K_L(N) \sim \frac{\Gamma\left(N + \frac{3}{2}(L-1)\right)}{\left(x_c^{3/2}C\right)^{L-1} \Gamma\left(\frac{3}{2}(L-1)x_c^N\right)}. \quad (40)$$

For the number of L-loop graphs weighted by their symmetry factors we may employ the following formulation of the SD equation:

$$\phi_L = \sum_{\{n_{p,q}\} \geq 0} V^{(m)} \prod_{p,q \geq 0} \frac{1}{(n_{p,q})!} \left(\frac{1}{(q+1)!}\phi_p^{(q)}\right)^{n_{p,q}},$$

$$(41)$$

where the bracketed superscripts denote derivatives, and

$$\sum_{p,q} (p+q)n_{p,q} = L, \quad m = 1 + \sum_{p,q}(q+1)n_{p,q}. \quad (42)$$

The successive expressions for $\phi_L(x)$ in terms of lower-loop ones can straightforwardly be worked out. For $L = 1, 2$ these have been given in the previous section. If we now put in the approximate form of $\phi_0(x)$ given in (10), it is easily checked (at least up to $L = 10$) that the expression for W is reproduced. Note that in this approximation the fourth and higher derivatives of $V(\phi_0)$ vanish, so that (41) is actually more complicated than need be: nevertheless, by using the next-to-leading expression

$$\phi_0(x) \sim \phi_c - C(x_c - x)^{1/2} - C'(x_c - x), \quad (43)$$

it can also be checked that, indeed, the subleading behavior of $\phi_0(x)$ shows up only in the subleading terms in $K_L(N)$. We conclude that *as $N \to \infty$, the average symmetry factor of any Feynman diagram approaches unity.*

5 Complexity of the Caravaglios–Moretti algorithm

5.1 Introduction

The CM algorithm, as first explicitly given in [1] (and earlier implied by [7]), consists of the computation of subamplitudes with one off-shell leg, the other legs corresponding to on-shell external legs of the transition matrix element. For tree diagrams, these subamplitudes can be unambiguously specified by the particular set of external momenta involved because of momentum conservation. For detailed descriptions, we refer to [1,6,8]: here, we are only interested in the combinatorics of the algorithm.

5.2 Complexity for tree level computations in any theory

We assume an N-particle process, and set $K = N-1$. Each subamplitude can then be encoded by a binary string with N bits, each referring to a given external particle. The bit is set to 1 if its external leg is involved in the subamplitude, and to 0 otherwise. For instance, the string $(1, 1, 0, 1, 1, 0, 0, 0, \ldots, 0, 0)$ denotes that subamplitude in which the external particles with labels 1, 2, 4 and 5 are combined, using the vertices of the theory, into a single off-shell momentum. By the same convention, a string with a single 1 refers to the Feynman rule for a single external particle (a spinor or antispinor for fermions, a polarization vector for vector particles, et cetera). The CM algorithm combines
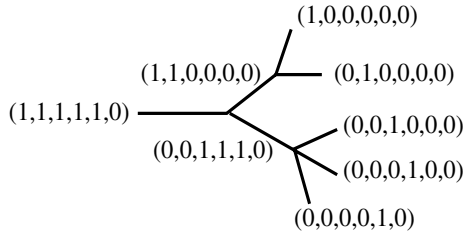
Fig. 2. Example of decomposition of string of K bits

subamplitudes into successively more complicated ones, culminating in the string $(1, 1, 1, \ldots, 1, 1, 1, 0)$, which, after multiplying with the external factor $(0, 0, 0, \ldots, 0, 0, 0, 1)$ gives the final answer for the amplitude. It is clear that of the N external particles, one can be left out of the combinatorics since it has to be included only at the very end. The combinatorial problem is, therefore, to determine the number of ways to decompose a string of K bits. An example of a possible decomposition is in Fig. 2. In this figure we have indicated the strings corresponding with the external legs and the various subamplitudes. The possible decompositions depend on the theory in question: the presence of an $(m+1)$-point vertex in the theory allows for a decomposition into m smaller strings. In this paper, we shall only deal with theories of a single self-interacting field (gluonic QCD being an example): extensions to more fields are fairly straightforward. In recent implementations such as HELAC ([9]), this decomposition can be recognised explicitly.

Let us first consider a subamplitude's string with n 1's being decomposed into m smaller strings, each with at least one 1. This happens when, in the SD equation, an $(m+1)$-point vertex is encountered. The number of inequivalent decompositions, denoted by $c_m(n)$, is given by

$$c_m(n) = \frac{1}{m!} \sum_{n_1, 2, \ldots, m \geq 1} \frac{n!}{n_1! \, n_2! \, \ldots \, n_m!} \,, \qquad (44)$$

where, of course, $n_1 + n_2 + \ldots + n_m = n$. Note that the above equation assumes that all the subamplitudes containing $n_1, n_2, \ldots, n_m$ external momenta exist. This is always the case when a φ^3 interaction is present in the theory[5] but it is not true for a pure φ^4 theory for example. Then one has to introduce a factor that cancels the terms coming from combinations of non-allowed subamplitudes. We, nevertheless, proceed with our program to find a generating function for effective theories that always contain a 3-point vertex. We find

$$\sum_{n \geq 0} \frac{x^n}{n!} c_m(n) = \frac{1}{m!} \left(e^x - 1 \right)^m \,. \qquad (45)$$

Now, out of all bit strings of size K, there are precisely $K!/n!(K-n)!$ strings containing precisely n 1's. The total

---

[5] Because then there is always the possibility of constructing a subamplitude containing n_k external momenta by combining a subamplitude containing $n_k - 1$ momenta with an external momentum in a 3-point vertex.

number of decompositions involving $(m+1)$-point vertices is therefore

$$f_m(K) = \sum_{n \geq 0} \binom{K}{n} c_m(n) \,, \qquad (46)$$

so that

$$g_m(x) \equiv \sum_{K \geq 0} \frac{x^K}{K!} f_m(K) = \frac{1}{m!} e^x \left(e^x - 1 \right)^m \,. \qquad (47)$$

In the simple case of a pure φ^3 theory we therefore have

$$g_2(x) = \frac{1}{2} \left(e^{3x} - 2e^{2x} + e^x \right)$$

$$= \sum_{K \geq 0} \frac{x^K}{K!} \frac{1}{2} \left(3^K - 2^{K+1} + 1 \right) \,, \qquad (48)$$

so that the number of decompositions necessary to arrive at an N-point amplitude is given by

$$\frac{1}{6} 3^N - \frac{1}{2} 2^N + \frac{1}{2} \,.$$

For a theory with both φ^3 and φ^4 interactions such as gluonic QCD, we find a total of

$$\frac{1}{24} 4^N - \frac{1}{4} 2^N + \frac{1}{3}$$

decompositions. In QCD at the tree level, an improvement is possible. We can decompose the gluonic 4-vertex into two 3-vertices by employing an auxiliary field, as explained for instance in [6]. This brings the complexity down from 4^N to 3^N, a worthwhile improvement for large N. It is not to be expected, however, that this will be possible in higher orders. The effective action, therefore, will contain $(m+1)$-vertices for all $m \geq 2$, and the generating function is therefore

$$F(x) = \sum_{m \geq 2} g_m(x) = \exp \left(e^x - 1 + x \right) - \exp(2x) \,. \qquad (49)$$

In Table 13 we give the number of decompositions,

$$D(N) = \sum_{m \geq 2} g_m(N-1) \,, \qquad (50)$$

for not-too-large values of N. For asymptotically large values of N, we have to study the analytic structure of $F(x)$. Since this function is analytic for finite x, $D(N)$ must increase with N slower than $N!$. On the other hand, $D(N)$ increases faster than c^N for any finite c, which is reasonable since as N grows, larger and larger values of m come into play. This is also evident from the fact that the standard Borel transform of the series $F(x)$,
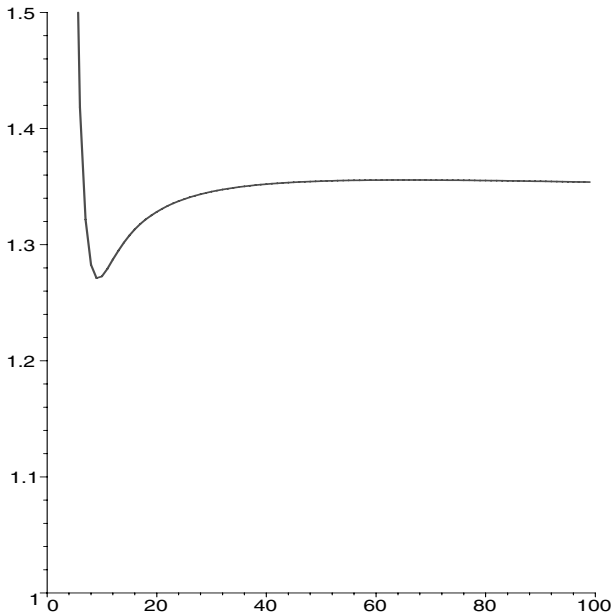
Fig. 3. The ratio $\frac{\log(N)/N}{D(N)/D(N-1)}$ as a function of N for $3 \leq N \leq 100$

$$\int\limits_0^\infty \mathrm{d}y \; \mathrm{e}^{-y} \; F(xy)$$

$$= -\frac{1}{1-2x} + \int\limits_0^\infty \mathrm{d}y \; \exp\left(-y + \mathrm{e}^{xy} - 1 + xy\right), \quad (51)$$

does not converge for any positive value of x. Figure 3 shows the behavior of the ratio

$$\frac{\log(N)/N}{D(N)/D(N-1)}$$

as a function of N for $3 \leq N \leq 100$. For high N, this ratio is approximately (but not quite) a constant.

5.3 Complexity in one and two loops

Consider a general theory with m-point vertices. Each subamplitude of level n (containing n specific external momenta), can be constructed by combining 2- or more lower-level subamplitudes in a 3- or more-point vertex. When using an $(m+1)$-point vertex the subamplitude is

Table 13. Number of decompositions, $D(N) = \sum\limits_{m \geq 2} g_m(N-1)$, for not-too-large values of N

N	$D(N)$	N	$D(N)$
3	1	8	4,012
4	7	9	20,891
5	36	10	115,460
6	171	11	677,550
7	813	12	4,211,549

built by m lower-level subamplitudes and the number of different ways for this to happen is given by (44).

Each term in the series represents the number of ways to construct the subamplitude of level n using subamplitudes of level $n_1, \ldots, n_m$. The computational cost of each such subamplitude involves (assuming that there is an $m+1$-vertex in the theory) contributions from the following possibilities: All lower subamplitudes are free of loop corrections and the vertex is an ordinary one (this gives the tree level subamplitude)[6]. It can also be that one of the subamplitudes contains already a loop correction (this occurred in previous steps in the C.M. algorithm) and the vertex is an ordinary one (see (52)). The subamplitudes containing loop corrections can, however, be of level 2 or higher since the level one subamplitudes are the external legs which we consider amputated. There are, therefore, $m - \sum_i \delta_{1,n_i}$ different possibilities. Finally there is the case that all subamplitudes are free of loop corrections but the vertex is actually a loop (see the last term in (52)). The number of different possibilities is now equal to the number of 1PI diagrams with one loop and $m+1$ legs, which we denote by $J_{m,1}$.

$$(52)$$

The cost of computing the specific subamplitude via an $m+1$-vertex is therefore

$$\frac{1}{m!} \sum_{\substack{n_1,\ldots,n_m \\ \sum n_i = n}} \frac{n!}{n_1! n_2! \ldots n_m!} \left(V_m \left(1 + m - \sum_i \delta_{1,n_i}\right) + J_{m,1} \right),$$
$$(53)$$

where we have included a factor $V_m = 1$ if the $m+1$-vertex is in the theory and $V_m = 0$ if not. The cost of the subamplitude is then found by summing over m. There are $\frac{(N-1)!}{n!(N-1-n)!}$ different subamplitudes. The computational cost of the whole algorithm in units of effective vertices is then

$$\sum_{n=2}^K \binom{K}{n} \sum_{m \geq 2}^\infty \frac{1}{m!} \qquad (54)$$

$$\times \sum_{\substack{n_1,\ldots,n_m \\ \sum n_i = n}} \frac{n!}{n_1! \ldots n_m!} \left(V_m \left(1 + m - \sum_i \delta_{1,n_i}\right) + J_m \right),$$

where $K = N - 1$. In Table 14 we present the results for the four test theories.

---

[6] That is, provided that the lower-level subamplitudes exist! This always happens when the theory involves φ^3 interactions. In the pure φ^4 theory, however, we have to modify the calculation to exclude combinations where one of the n_i's is equal to 2 since in such a theory there are no level 2 subamplitudes.

Table 14. Results from (54)

	φ^3	φ^4	$\varphi^3 + \varphi^4$	effective
$N = 1$	0	0	0	0
$N = 2$	0	0	0	0
$N = 3$	2	0	5	6
$N = 4$	18	4	46	57
$N = 5$	114	0	340	442
$N = 6$	720	105	2,715	3,713
$N = 7$	5,368	0	26,346	37,411
$N = 8$	49,686	3,395	315,035	459,056
$N = 9$	553,766	0	4,474,868	6,688,320
$N = 10$	7,112,700	149,140	72,741,355	112,139,709

Table 15. Results after adding the number of 1PI graphs with two loops and $m + 1$ legs, $J_{m,2}$

	φ^3	φ^4
$N = 1$	0	0
$N = 2$	0	0
$N = 3$	9	0
$N = 4$	102	16
$N = 5$	957	0
$N = 6$	9,740	610
$N = 7$	114,677	0
$N = 8$	1,546,986	32,151
$N = 9$	23,395,461	0
$N = 10$	390,310,512	2,574,670

	$\varphi^3 + \varphi^4$	effective
$N = 1$	0	0
$N = 2$	0	0
$N = 3$	45	68
$N = 4$	566	857
$N = 5$	6,414	9,837
$N = 6$	81,560	127,451
$N = 7$	1,201,556	1,920,824
$N = 8$	20,211,345	33,181,094
$N = 9$	380,938,056	644,468,452
$N = 10$	7,929,937,496	13,861,514,611

In order to include the 2-loop correction one has to add to the above formula a term $(m - \sum \delta_{1,n_i}) (m - \sum \delta_{n_i} - 1)$ for the possibility that two of the lower subamplitudes have a 1-loop correction and a term equal to $m - \sum \delta_{1,n_i}$ for the possibility that one of the subamplitudes has a 2-loop correction. There is also the possibility that one of the lower subamplitudes is of 1-loop order and the vertex itself is a 1-loop 1PI graph. This costs an extra term $J_{m,1} (m - \sum \delta_{1,n_i})$. Moreover one has to add the number of 1PI graphs with two loops and $m + 1$ legs, $J_{m,2}$. Hence we now have, writing $S_{n_i} = \sum_i \delta_{1,n_i}$,

$$\sum_{n=2}^{K} \binom{K}{n} \sum_{m \geq 2}^{\infty} \frac{1}{m!} \sum_{\substack{n_1,\ldots,n_m \\ \sum n_i = n}} \frac{n!}{n_1! \ldots n_m!} (A + B + C),$$

Table 16. Ratios for a calculation in tree, tree plus 1-loop, and tree plus 1- and 2-loop level

complexity of C.M. algorithm /

		number of diagrams	
		φ^3	
	L_0	$L_0 + L_1$	$L_0 + L_1 + L_2$
$N = 3$	1.00	1.000	1.500
$N = 4$	2.00	1.200	1.307
$N = 5$	1.666	0.864	0.955
$N = 6$	0.857	0.516	0.679
$N = 7$	0.318	0.309	0.498
$N = 8$	0.093	0.199	0.375
$N = 9$	0.022	0.136	0.286
$N = 10$	0.005	0.095	0.220

		φ^4	
	L_0	$L_0 + L_1$	$L_0 + L_1 + L_2$
$N = 3$	–	–	–
$N = 4$	1.000	1.000	1.231
$N = 5$	–	–	–
$N = 6$	2.00	1.235	1.119
$N = 7$	–	–	–
$N = 8$	1.575	0.858	0.819
$N = 9$	–	–	–
$N = 10$	0.636	0.468	0.584

		$\varphi^3 + \varphi^4$	
	L_0	$L_0 + L_1$	$L_0 + L_1 + L_2$
$N = 3$	1.000	1.000	1.363
$N = 4$	1.500	1.070	1.132
$N = 5$	1.00	0.736	0.828
$N = 6$	0.409	0.451	0.605
$N = 7$	0.121	0.283	0.454
$N = 8$	0.028	0.190	0.347
$N = 9$	0.005	0.132	0.268
$N = 10$	0.001	0.094	0.208

		effective	
	L_0	$L_0 + L_1$	$L_0 + L_1 + L_2$
$N = 3$	1.000	1.200	1.619
$N = 4$	1.500	1.212	1.325
$N = 5$	0.961	0.837	0.956
$N = 6$	0.381	0.519	0.691
$N = 7$	0.109	0.327	0.515
$N = 8$	0.025	0.217	0.392
$N = 9$	0.005	0.150	0.302
$N = 10$	0.001	0.107	0.234

where $K = N - 1$ and

$$A = V_m(1 + m - S_{n_i}$$
$$+ (m - S_{n_i})(m - S_{n_i} - 1) + m - S_{n_i}),$$
$$B = J_{m,1} + J_{m,1}(m - S_{n_i}),$$
$$C = J_{m,2}.$$

The results for the four test cases are presented in Table 15.

One should be aware of the fact that the above results are obtained under the assumption that the computational cost for every effective vertex that might include 1- or 2-loop 1PI graphs is the same.

6 Comparison of the complexity of the C.M. algorithm to the diagrammatic approach

We present below the ratio of the computational complexity of the C.M. algorithm over the number of diagrams one has to calculate in the customary diagrammatic approach, for our four test theories[7]. For each case the ratio for a calculation in tree, tree plus 1-loop, and tree plus 1- and 2-loop level is presented in Table 16.

One should note that the C.M. algorithm will actually perform better than depicted by the above numbers, when compared with the straightforward diagrammatic approach, since we consider the cost of a step in the C.M. algorithm (i.e. the calculation of a subamplitude which corresponds to the calculation of an effective vertex) equal to the cost of the computation of a whole diagram. That is the reason for the apparently poor performance of the C.M. algorithm in the case of tree level φ^4 theory.

We, therefore, conclude that the Caravaglios–Moretti algorithm is more effective than the straightforward diagrammatic approach, in the tree as well as the 1- and 2-loop level, by a factor that increases rapidly with the number of external legs, even though this increase is less rapid in the 1- and 2-loop level than in tree level.

References

1. F. Caravaglios, Mauro Moretti, Phys. Lett. B **358**, 332 (1995) [hep-ph/9507237]
2. P.D. Draggiotis, R. Kleiss, Eur. Phys. J. C **23**, 701 (2002) [hep-ph/0110225]
3. P.D. Draggiotis, R. Kleiss, Eur. Phys. J. C **24**, 447 (2002) [hep-ph/0202201]
4. P.D. Draggiotis, R. Kleiss, Eur. Phys. J. C **27**, 291 (2003) [hep-ph/0209155]
5. P. Cvitanovic̀, B. Lautrup, R.B. Pearson, Phys. Rev. D **18**, 1937 (1978)
6. Petros D. Draggiotis, Exploding QCD, Ph.D. thesis (Nijmegen University) (2003)
7. F.A. Berends, W.T. Giele, Nucl. Phys. B **306**, 759 (1988)
8. P.D. Draggiotis, R. Kleiss, C.G. Papadopoulos, Phys. Lett. B **439**, 157 (1998) [hep-ph/9807207]
9. A. Kanaki, C.G. Papadopoulos, Comput. Phys. Commun. **132**, 306 (2000) [hep-ph/0002082]

---

[7] Only amputated, tadpole/seagull-free diagrams are considered.